Real-Time User-Independent Slope Prediction Using Deep Learning for Modulation of Robotic Knee Exoskeleton Assistance

Dawit Lee, Inseung Kang, Dean D. Molinaro, Alexander Yu, and Aaron J. Young

Abstract—Ground slope incline is a critical environmental variable that influences exoskeleton control parameters since human biological joint demand is correlated to changes in slope incline. Current literature methods take a heuristic approach by numerically calculating the slope incline from on-board mechanical sensors. However, these methods often require a user-specific tuning procedure and are prone to noise and sensor drift when tested in a dynamic setting, such as overground locomotion. In this study, we propose the use of a deep learning slope prediction model capable of generalizing across users and terrain. To evaluate this approach, we collected training data (N = 10) and utilized a convolutional neural network to predict the inclination angle and actively modulate the peak assistance magnitude of a bilateral robotic knee exoskeleton in real-time. From online validation results (N = 3), our model predicted the slope incline with an average RMSE of 1.5° during treadmill and overground walking. Furthermore, our model accurately predicted the slope incline in the extrapolated region outside of the training data with an average RMSE of 1.7° during treadmill and overground walking. Our study's findings showcase the feasibility of using deep learning models to actively modulate exoskeleton assistance, translating this technology to more realistic locomotion environments.

Index Terms—Convolutional neural network, deep learning, robotic knee exoskeleton, slope prediction.

I. INTRODUCTION

XOSKELETON technology holds great promise for improving human mobility. The effectiveness of using these exoskeletons for augmenting human locomotion has been investigated in various applications [1]–[3]. Several literature studies have demonstrated successful results in human augmentation during locomotion with exoskeleton assistance, such as reducing

Manuscript received October 15, 2020; accepted February 26, 2021. Date of publication March 17, 2021; date of current version April 6, 2021. This letter was recommended for publication by Associate Editor T. Lenzi and Editor P. Valdastri upon evaluation of the reviewers' comments. This work was supported in part by the Shriner's Foundation, the NSF NRI Award #1830215, in part by the NextFlex NMMI Grant under Award PC3.6 – LMCOGaTech, the NSF GRFP Award #DGE-1650044, and in part by the NRT: Accessibility, Rehabilitation, and Movement Science (ARMS) Award #1545287. (Corresponding author: Dawit Lee.)

Dawit Lee, Inseung Kang, and Alexander Yu are with the School of Mechanical Engineering, Georgia Institute of Technology, Atlanta, GA 30332 USA (e-mail: dlee444@gatech.edu; ikang7@gatech.edu; ayu64@gatech.edu).

Dean D. Molinaro and Aaron J. Young are with the School of Mechanical Engineering, Georgia Institute of Technology, Atlanta, GA 30332 USA, and also with the Institute for Robotics and Intelligent Machines, Georgia Institute of Technology, Atlanta, GA 30332 USA (e-mail: dmolinaro3@gatech.edu; aaron.young@me.gatech.edu).

Digital Object Identifier 10.1109/LRA.2021.3066973

the metabolic cost of walking [4]–[7]. Additionally, these studies have shown that the user's benefit is influenced by varying exoskeleton control parameters, such as the desired assistance level, which is often directly correlated with the user's biological demand. [8]–[10].

The knee joint exhibits an increase in biological joint moment with an increase in slope incline during incline walking [11]. Therefore, to maintain maximal human-exoskeleton performance across different slopes, active modulation of the exoskeleton assistance level depending on the ground slope incline is needed. However, current literature methods are only evaluated at a static slope incline setting and have not explored the feasibility of translating to dynamic incline settings [12], [13]. Thus, to translate this exoskeleton technology to a real-world scenario, such as an outdoor terrain where the ground slope incline dynamically changes, a robust slope predictor that can adapt to different terrain settings is required to actively modulate the exoskeleton assistance.

Previously, different methods have been introduced in the literature to estimate ground slope incline. One common method is to estimate the slope incline by numerically integrating acceleration data from an inertial measurement unit (IMU) mounted to the shank or foot [14]–[16]. However, these methods are sensitive to sensor drift and may bias the estimated incline. Moreover, these methods rely on the cyclical nature of walking to determine the initial conditions for numerical integration or reset accumulated drift. However, in a real-world walking scenario where ground slope incline can dynamically change, the assumption of cyclical walking is not valid anymore, and these IMU integration-based methods may be unsuitable. Indeed, studies of slope estimation using IMU integration have thus far only been tested on static inclines. Other ground slope estimation techniques measure joint angles and segment orientation with mechanical sensors. Using these angles, the ground slope is calculated with geometric relations [17], [18]. In addition to joint angles, Shim et al. uses a pressure sensor to locate the center of pressure at the foot, and ground slope is calculated using the normal vector [19]. Sup et al. forgoes measuring joint angles entirely, instead using an IMU to directly measure the foot's tilt based on the components of gravitational acceleration for a knee-ankle powered prosthetic [20]. While these approaches suffer less from drift issues and can adapt to varying slopes, they are not without drawbacks. All existing slope estimation techniques update ground slope estimation after heel strike. [14]–[20].

Current approaches inherently limit the system to after-thefact slope estimation which can induce delay in updating exoskeleton control parameters. For instance, knee exoskeleton controllers deliver large torque assistance during early stance,

2377-3766 © 2021 IEEE. Personal use is permitted, but republication/redistribution requires IEEE permission. See https://www.ieee.org/publications/rights/index.html for more information.

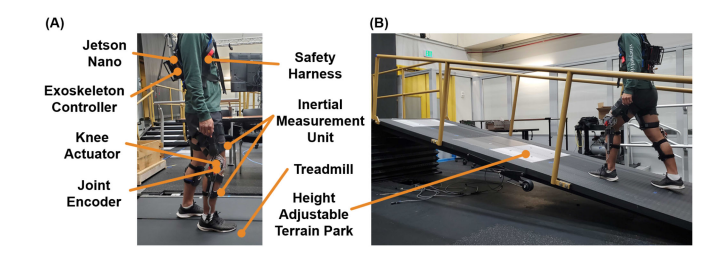


Fig. 1. (A) Autonomous bilateral robotic knee exoskeleton. The exoskeleton uses multiple mechanical sensors to record the user's limb kinematics. Additionally, the Jetson co-processor predicts the ground slope in real-time. (B) Real-time control of the knee exoskeleton during overground incline walking is shown using the height adjustable terrain park.

immediately after heel strike. Slope estimation techniques that require sampling sensor data after heel strike would delay the required assistance update for the controller. Machine learning (ML) techniques can mitigate the limitations of these analytical approaches. Previous literature studies in the wearable robotics field have used several machine learning techniques for inference during various locomotor estimation tasks [21]-[27]. The majority of these ML approaches utilize multiple mechanical sensors on the device to improve the robustness of the estimator via sensor fusion. This approach extracts feature information from each sensor to accurately estimate the desired locomotor variable. While there are several ML approaches that have been explored in the field, neural networks have recently gained attention from different groups due to their success in approximating high-dimensional functions for complex tasks. Most of the ML models in these studies yield compelling results, but are often trained on a user-specific basis, which is likely infeasible for real-world deployment.

The main objective of this study was to develop and validate a novel ground slope predictor that can actively modulate the knee exoskeleton assistance magnitude independent of the user. We utilized a sensor fusion approach using on-board mechanical sensors to train a deep convolutional neural network (CNN)-based model from ten able-bodied subjects. CNNs have previously been used for many upper-limb kinematic recognition tasks [28]-[30]. Using our optimized model from an offline analysis, we evaluated our model performance for both treadmill and overground walking in multiple slope inclines with three able-bodied subjects, randomly chosen from the subject group for the initial training collection. The user-independent model for each test subject was trained using the entire data set excluding the data set of each test subject. Our findings from this study showcase the future direction of ML-based exoskeleton control and the feasibility of translating this technology to more realistic settings.

II. SLOPE PREDICTION

A. Robotic Knee Exoskeleton

Our study utilized a single degree-of-freedom, light-weight, bilateral robotic knee exoskeleton that we recently developed, capable of providing assistance torque in flexion and extension (Fig. 1) [31]. The exoskeleton uses several on-board mechanical sensors: 1) an absolute knee joint encoder (angular position and velocity), 2) 6-axis inertial measurement units (IMUs) mounted on the shank and thigh cuffs (accelerometer and gyroscope), and 3) two force sensitive resistors (FSRs) placed at the user's

heel of each leg. The exoskeleton, running fully autonomously, has an overall mass of 4.3 kg, including a 1.3 kg control box and can generate a peak torque of 17.4 Nm. For this study, the exoskeleton control loop and mechanical sensor data logging were executed at 100 Hz on a microprocessor (myRIO, National Instruments, USA). We implemented an additional co-processor to the system for running real-time slope inference (Jetson Nano, NVIDIA, USA). Data was transferred between the co-processor and exoskeleton controller through an ethernet cable via TCP/IP communication protocol.

B. Exoskeleton Torque Controller

Our knee exoskeleton utilized a torque controller that generated knee extension assistance during the early stance phase (0~30%) of the gait cycle [31]. The user's heel strike was detected using a force sensitive resistor (FSR) placed at the user's heel. Using this gait event marker, we estimated the user's gait phase, t_i , using a time-based estimation method that computed the quotient between the time since last heel strike and the user's average stride duration [32]. Given a peak assistance magnitude, τ_{peak} , and assistance duration, t_d , the torque command, τ_i , was updated using a parabola scaled to the desired target peak assistance magnitude as a function of t_i (1).

$$\tau_i = \begin{cases} \frac{\tau_{peak} \times t_i \times (t_d - t_i)}{(0.5 \times t_d)^2} & 0 \le t_i \le t_d \\ 0 & t_d \le t_i \end{cases}$$
 (1)

In this study, t_d was fixed to 30% of the gait cycle to provide exoskeleton assistance through early stance. The exoskeleton remained unpowered for the remainder of the gait cycle.

C. Initial Training Data Collection

We recruited ten able-bodied adults (4 females/6 males, mean \pm standard deviation, 22.2 \pm 3.5 years, 173.1 \pm 8.6 cm, and 68.7 ± 8.5 kg) after providing informed written consent. Our study was approved by the Georgia Institute of Technology Institutional Review Board. All subjects were asked to walk on a treadmill wearing the bilateral knee exoskeleton at a constant walking speed of 1.0 m/s. Subjects walked at various inclination levels starting from 0° to 10° of inclination at 2° increments and walked for 2 minutes at each inclination level. Before the subject started the first walking condition, level-ground, the angle reading of the encoder was initialized to 0° and was not re-initialized again throughout the data collection. The early stance phase is where the knee undergoes positive power generation through an extension moment during slope walking [11]. Thus, the exoskeleton provided knee extension assistance during the early stance phase of the gait cycle on both legs using the exoskeleton torque controller. The peak assistance magnitude, τ_{peak} , was modulated based on the inclination level (s), such that au_{peak} was 1 Nm at 0° and was linearly increased by 1 Nm for every 2° increment in slope, as shown in (2).

$$\tau_{peak} = 0.5s + 1 \tag{2}$$

This was based on the increase in the knee joint's peak extension moment during early stance phase as inclination becomes steeper [11]. Throughout the trials, all mechanical sensor data from the right leg (knee joint encoder and shank and thigh IMUs) were recorded for training the model.

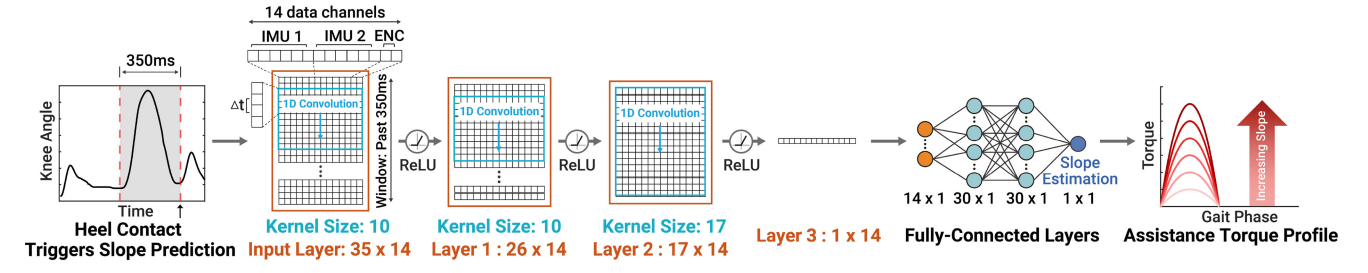


Fig. 2. Convolutional Neural Network-based slope predictor for controlling the robotic knee exoskeleton. Raw mechanical sensor data over 350 ms is input to the CNN model to predict the ground slope at heel contact during walking. The predicted slope updates the targeted knee assistance peak torque to adapt the exoskeleton assistance to the inclination. Each hidden node of the fully-connected layers is activated using the ReLU function.

D. Convolutional Neural Network Model Optimization

We implemented a deep Convolutional Neural Network (CNN), using three 1-dimensional convolutional layers and two fully connected layers, to estimate the ground inclination at each heel strike of the right leg (Fig. 2). CNNs remove the burden of pre-processing the input data compared to hand-engineered feature extraction and often learn better feature representations, resulting in improved model performance [33]. Additionally, CNNs reduce the number of learnable parameters compared to fully connected networks by localizing the connections in each layer as specified by the kernel shape, which reduces the likelihood of overfitting. The input sequence length to the model was fixed at 350 ms, which was selected to maximize the input sequence length during the swing phase of gait. This allowed for the maximum amount of information to be provided to the network without including previous stance phase data that could bias the estimate towards the previous ground inclination.

The forward pass of each convolutional layer of output channel, $a_j^{(l)}$, was computed using the learned filter $(z_j^{(l)})$ and bias $(b_{conv,j}^{(l)})$ and activated using the rectified linear unit (ReLU), where n is the number of input channels of the current layer (l), \star is the cross-correlation operator, and $a^{(0)}$ is the windowed exoskeleton sensor data, as shown in (3).

$$a_j^{(l)} = ReLU(b_{conv,j}^{(l)} + \sum_{i=0}^{n-1} z_{j,i}^{(l)} \star a_i^{(l-1)}), l = 1, 2, 3$$
 (3)

The two fully connected layers included after the convolutional layers were used to compute the estimated slope inclination $(\hat{s} \in \mathbb{R})$ using the learned feature representation from the convolutional layers. Thus, \hat{s} was computed using the weights $(w^{(l)})$ and biases $(b_{fc}^{(l)})$ of the fully connected layers and final output of the convolutional layers $(a^{(3)})$ as shown in (4) and (5).

$$a^{(4)} = ReLU(w^{(4)^T}a^{(3)} + b_{fc}^{(4)})$$
(4)

$$\hat{s} = w^{(5)^T} a^{(4)} + b_{fc}^{(5)} \tag{5}$$

We trained both user-dependent and user-independent slope prediction models for each subject using Python v3.7.1 and the deep learning package, Pytorch v1.4.0. The complete model architecture is shown in Fig. 2. Each model was trained using the RMSprop optimizer, with a learning rate of 0.0001 and a loss function computed as the root-mean-square error between the labeled and predicted inclination angles. Using the user-dependent method, models were trained using data specific to a single subject. 8-fold cross-validation with early stopping

criteria was used to prevent overfitting of the user-dependent models. The best performing model for each subject was then tested offline on 20% of the data, which was held-out during the cross-validation training. The user-independent models were trained using a leave-one-subject-out approach, in which each model was trained using the entire dataset excluding the test subject. These models were trained for 300 epochs without monitoring the test subject score to prevent biasing the model's performance on the test subject data. Each user-independent model was then evaluated on the novel subject data.

III. REAL-TIME VALIDATION

A. Experimental Protocol

To evaluate the online performance of our optimized userindependent slope prediction model, three subjects walked with the exoskeleton using our slope predictor. The range of tested slope conditions was chosen to include slopes within the training data of 0° to 10° (interpolation) and outside of the training data above 10° (extrapolation) to quantify the model's ability to recognize previously unseen slopes. First, the subject was asked to walk on a treadmill for 460 seconds while wearing the powered knee exoskeleton as the treadmill dynamically varied the ground slope between 0° to 14° at 1.0 m/s using a predefined slope profile. The slope initially started at 0°, was raised to 1°, increased to 13° in 2° increments, and reached 14°. Then, the slope eventually traveled back to 0° in 2° decrements. Afterwards, the subject was asked to walk on the overground inclined ramp (5.2°, 7.8°, 9.2°, 11°, 12.4°, and 18°) at their preferred walking speed. The CNN model updated the ground slope prediction at heel-contact of the right leg, which was used to scale the peak assistance magnitude in real-time for both legs using (2) during walking.

B. Data Analysis

The slope prediction root-mean-square error (RMSE) was computed using the difference between the ground-truth slope and the predicted slope from the CNN model. For online testing on overground walking, the RMSE for each slope was calculated by averaging the RMSE for each slope for each subject across the three subjects. The RMSE of interpolation and extrapolation were separately calculated by averaging across RMSEs for slopes less than or equal to 10° and slopes greater than 10° respectively. Since the training data was collected during treadmill walking, the data from treadmill walking were analyzed for both offline and online analysis. For the offline analysis of treadmill walking, the average RMSE of slopes for each subject was

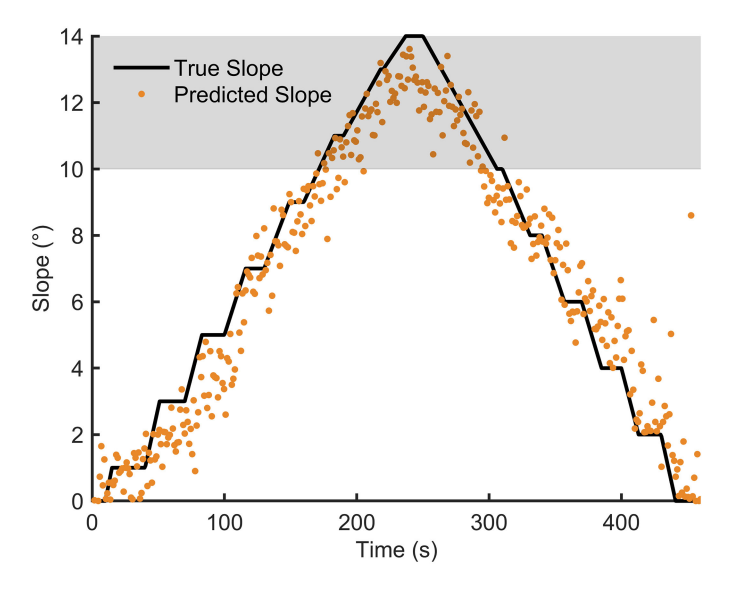


Fig. 3. Time series plot of a representative subject's real-time treadmill slope prediction instances (orange dots) with respect to the ground truth slope (black line). The shaded grey region indicates the extrapolation region, and the white region indicates the interpolation region.

separately averaged for both user-dependent and -independent models. A two-tailed paired t-test was used to determine the statistical difference between the offline test results of the user-dependent and user-independent training methods in RMSEs. The statistical test was conducted using SPSS Statistics 21.0 (IBM, Amonk, NY, USA) ($\alpha=0.05$). For overground walking, the transition step between the level ground and the inclined ramp was excluded for the analysis since the step involved turning at a right angle and the training data collected on the treadmill did not include turning. The data is presented as mean \pm standard error of mean (SEM).

IV. RESULTS

A. Overall Slope Prediction Performance

Our offline analysis resulted in a significant decrease in slope prediction RMSE by the user-dependent CNN compared to the user-independent model (p < 0.05). Specifically, the offline userdependent model resulted in a prediction RMSE of $0.61 \pm 0.05^{\circ}$, which was a 71.4% reduction compared to the user-independent offline RMSE of $2.15 \pm 0.29^{\circ}$. When deployed in real-time, the user-independent slope prediction model resulted in an average RMSE of $1.51 \pm 0.17^{\circ}$ during treadmill walking across all tested slopes (Fig. 3), which was similar to our offline result. Additionally, the user-independent model performed similarly in the overground condition with an overall RMSE of 1.58 \pm 0.17° (Fig. 4). Furthermore, the peak assistance magnitude in the exoskeleton torque profile was simultaneously updated and resulted in the overall RMSE of 0.75 \pm 0.13 Nm and 0.79 \pm 0.07 Nm during treadmill walking and over-ground walking, respectively (Fig. 5).

B. Generalizability of Slope Prediction

The online user-independent model generalized well to extrapolation tasks of previously unseen slopes (> 10°), with the largest average extrapolation RMSE of $2.09 \pm 0.30^{\circ}$ occurring

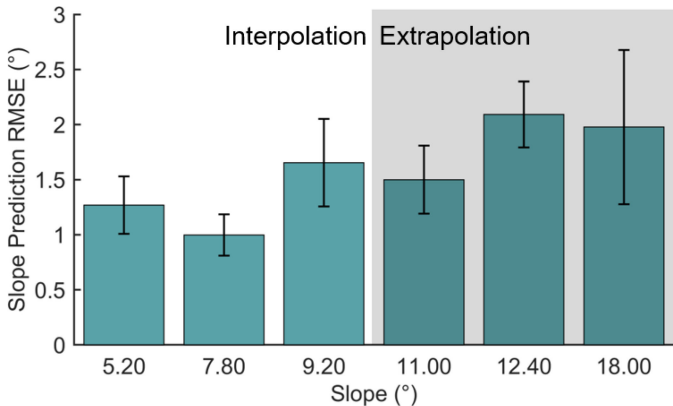


Fig. 4. RMSE for each overground slope. 5.2° , 7.8° , 9.2° are within the interpolation region, and 11° , 12.4° , and 18° are in the extrapolation region as shown by the gray shaded region. The model shows a relatively higher RMSE for the slope prediction during the extrapolation region than the interpolation region. The error bars show mean \pm 1 SEM.

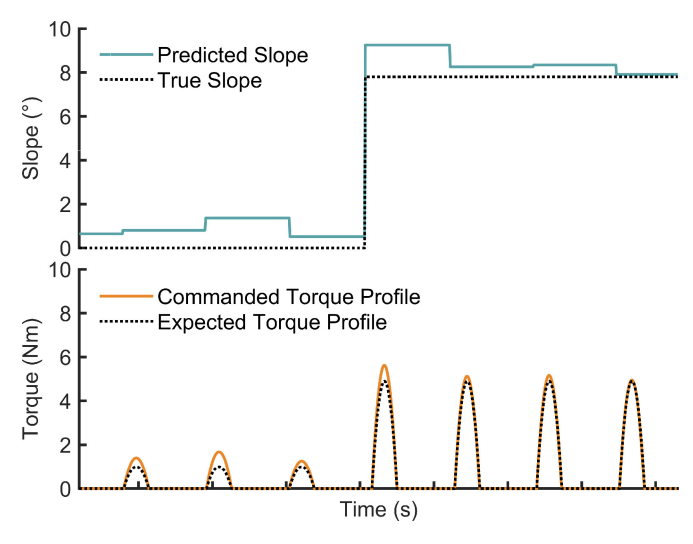


Fig. 5. Time series plot of the overground trial illustrating the accurate prediction of ground slope. The top shows the slope prediction in real-time and bottom shows the corresponding torque command generated from the slope prediction. Black dotted lines indicate the ground truth for slope and torque.

at the 12.4° overground condition (Fig. 4). When tested on the treadmill, the extrapolation conditions resulted in a 0.1° increase in slope prediction RMSE compared to the interpolation conditions (Fig. 6). The overground test yielded a similar result, as the extrapolation conditions increased the RMSE by 0.6° compared to the overground interpolation conditions.

V. DISCUSSION

On average, our CNN model predicted walking inclination within 2.1° across all offline and online test conditions. Our offline analysis showed that the user-dependent slope predictor resulted in an RMSE of $0.61 \pm 0.05^\circ$, which was significantly lower than the user-independent RMSE of $2.15 \pm 0.29^\circ$ (p < 0.05). The accuracy presented in this work showcases the use of a deep learning approach to predict the slope incline. The offline user-dependent model result in this paper outperformed our previous offline user-dependent neural network slope estimator using a hip exoskeleton, 1.4° RMSE [24]. Comparing

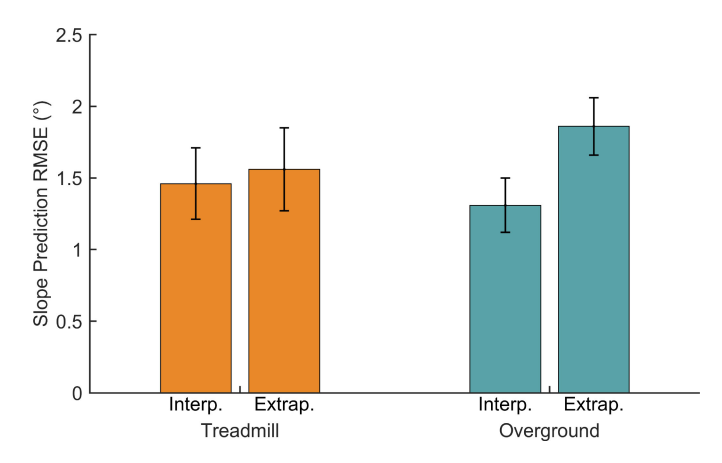


Fig. 6. Average RMSE comparison between interpolation and extrapolation during treadmill walking (orange) and overground walking (green). The error bars show mean \pm 1 SEM.

the accuracy to other methods, previous works integrating IMU signals for slope estimation, Sabatini *et al.* and Lopez *et al.* reported 0.87° and 2.86° [15], [16]. Additionally, the methods relying on joint angles and leg geometry Kim *et al.* and Zou *et al.* reported absolute slope estimation errors of 1.52° and 0.39°, respectively [17], [18]. While the accuracy our ML approach does not always outperform other methods, we emphasize that the strength and novelty of ML lies in its predictive power and ability to adapt to dynamically varying incline as a user-independent solution.

The user-dependent predictor performed significantly better than the user-independent model in our offline analysis. However, the user-dependent approach presents complications for real-world deployment given the need to collect subject-specific data. Conversely, the user-independent predictor is immediately ready for online deployment regardless of the user's anthropometry or gait patterns, which provides real-world viability for our exoskeleton controller. Specifically, no subject-specific data or sensor normalization was required during our online userindependent validation other than initializing the encoder angle during exoskeleton startup. Additionally, the user-independent model performed competitively during online testing (1.46° RMSE) compared to the offline result (2.15° RMSE) for 0 to 10° treadmill walking. This indicates that our initial data collection appropriately captured the variability in mechanical sensor data across users and that the kinematic patterns of the user's limbs described by the sensor data were globally generalizable across subjects. However, the offline result suggests that user-specific data can further improve accuracy and that self-adapting systems that learn user-specific gait patterns online could be beneficial.

The online performance validation of our user-independent predictor demonstrated reliable real-time prediction of ground slope incline. During treadmill walking, the incline RMSE between the interpolation and extrapolation region showed similar prediction performance with only a 0.1° difference in average RMSE. This result indicated that the ML model was capable of extrapolating the slope prediction outside of the slope ranges that were seen within the training data set, up to 40% of the range of training data for treadmill. Interestingly, the overground test showed a larger increase in RMSE of 0.6° between the interpolated and extrapolated conditions compared to the treadmill test; however, this larger increase may have been because the overground test included larger slope inclines, up to 18°, than

the treadmill result. Nevertheless, the prediction RMSE during the overground extrapolated conditions, 1.86° RMSE, was still below the RMSE produced by our offline analysis and suggests that our slope prediction model appropriately generalized to a wide range of slopes up to 80% larger than those included in the training data. This result also indicates the feasibility of using a model trained on treadmill-based data, which is easy to collect and label, for slope prediction during overground walking, which is more representative of community locomotion. One possible explanation for this result is that the subject's treadmill walking speed might have been representative of their self-selected overground walking speed, especially since the average adult's preferred walking speed at a 7° inclined surface is 1.0 m/s [34], which was the walking speed on the treadmill for this experiment. Therefore, walking at similar speeds between the training and test data may be an important consideration for developing future ML-based estimators for gait variables. Another interesting result observed from the overground trial was at the maximum incline setting (18°). The observed joint kinematics during an uphill walking at an extreme incline was more representative of stair ascent [35], [36]. Given that our maximum testing condition was comparably steep, we expected that our slope predictor performance would start to degrade as the user's gait dynamics would start to deviate further from the ones seen in the training data set. However, our ML model only had an RMSE increase of 0.67° from the interpolation region illustrating the power of neural network in generalizing the prediction slopes which would not have been possible using a conventional heuristic method shown in the literature.

There were several limitations of the study that can be addressed in the future to improve the performance of the slope prediction model. 1) The training data was collected from ten ablebodied adults. Given that we used a user-independent method for this study, the performance of the model may have been improved if we collected the training data from a larger number of participants. 2) The training data was only collected during steady-state walking on a treadmill. It is likely that including gait mode transitions and varied walking speeds will improve the performance and generalizability of the slope prediction model. 3) Similarly, we trained and tested our model using a single exoskeleton controller. Future research should explore the generalizability of the slope estimator to changes in exoskeleton control, such as changes in magnitude or assistance shape, especially if the controller changes user leg swing dynamics. 4) Our study only investigated slope prediction during incline walking. This work should be extended to include decline walking and could likely be applied to the prediction for other continuous gait environment variables, such as the stair height. It is possible that other neural network variants, such as a many-to-one LSTM model, that do not rely on a constant input window size may also be well-suited for this task; however, these models would require additional toe-off sensing to reinitialize the hidden/cell states for each new swing phase, which our current device does not include.

Our study was also limited by the low number of subjects that participated in the online validation of our slope prediction-based controller. Additionally, our study limited the scope of analysis to evaluating the accuracy and generalizability of the slope prediction model. Also, due to the limitation in the walking platform, the range of slope tested for treadmill and overground was different. Future studies should investigate the impact in human biomechanical outcomes of using this controller during various locomotion tasks.

VI. CONCLUSION

This study presented the design and real-time validation of a novel user-independent slope prediction model used to scale assistance magnitude of a bilateral knee exoskeleton. Our model used a deep convolutional neural network to predict the ground slope using multiple mechanical sensors on-board the exoskeleton, resulting in accurate real-time slope prediction across a wide variety of inclines during both treadmill and overground locomotion, with an overall RMSE of 1.51 \pm 0.17° and 1.58 $\pm 0.17^{\circ}$, respectively. We tested our system online under slope conditions within and outside the range of slopes in the training data and found that the model sufficiently generalized slope prediction to extrapolation tasks with a maximum RMSE of 2.1°, which is an improvement from comparable systems in the literature. Therefore, our study introduces and evaluates a completely autonomous, end-to-end exoskeleton system capable of adjusting assistance magnitude with respect to changes in biological joint demand. This is an exciting step towards autonomous exoskeleton solutions for real-world community ambulation.

ACKNOWLEDGMENT

The authors thank the subjects who participated in the study. The authors also acknowledge Pratik Kunapuli and Bailey McLain for help with the initial study design.

REFERENCES

- G. S. Sawicki, O. N. Beck, I. Kang, and A. J. Young, "The exoskeleton expansion: Improving walking and running economy," *J. NeuroEngineering Rehabil.*, vol. 17, no. 1, pp. 1–9, 2020.
- [2] T. Zhang and H. Huang, "A lower-back robotic exoskeleton: Industrial handling augmentation used to provide spinal support," *IEEE Robot. Automat. Mag.*, vol. 25, no. 2, pp. 95–106, Jun. 2018.
- [3] A. J. Young and D. P. Ferris, "State of the art and future directions for lower limb robotic exoskeletons," *IEEE Trans. Neural Syst. Rehabil. Eng.*, vol. 25, no. 2, pp. 171–182, Feb. 2017.
- [4] D. Lee, E. C. Kwak, B. J. McLain, I. Kang, and A. J. Young, "Effects of assistance during early stance phase using a robotic knee orthosis on energetics, muscle activity, and joint mechanics during incline and decline walking," *IEEE Trans. Neural Syst. Rehabil. Eng.*, vol. 28, no. 4, pp. 914–923, Apr. 2020.
- [5] A. J. Young, H. Gannon, and D. P. Ferris, "A biomechanical comparison of proportional electromyography control to biological torque control using a powered hip exoskeleton," *Front. Bioeng. Biotechnol.*, vol. 5, pp. 1–17, Jun. 2017.
- [6] Y. Ding, M. Kim, S. Kuindersma, and C. J. Walsh, "Human-in-the-loop optimization of hip assistance with a soft exosuit during walking," *Sci. Robot.*, vol. 3, no. 15, 2018, Paper eaar5438.
- [7] J. Zhang et al., "Human-in-the-loop optimization of exoskeleton assistance during walking," Science, vol. 356, no. 6344, pp. 1280–1284, 2017.
- [8] I. Kang, H. Hsu, and A. Young, "The effect of hip assistance levels on human energetic cost using robotic hip exoskeletons," *IEEE Robot. Automat. Lett.*, vol. 4, no. 2, pp. 430–437, Apr. 2019.
- [9] B. Quinlivan *et al.*, "Assistance magnitude versus metabolic cost reductions for a tethered multiarticular soft exosuit," *Sci. Robot*, vol. 2, no. 2, pp. 1–10, 2017.
- [10] S. Galle, P. Malcolm, S. H. Collins, and D. De Clercq, "Reducing the metabolic cost of walking with an ankle exoskeleton: Interaction between actuation timing and power," *J. Neuroeng. Rehabil.*, vol. 14, no. 1, p. 35, 2017.
- [11] J. R. Montgomery and A. M. Grabowski, "The contributions of ankle, knee and hip joint work to individual leg work change during uphill and downhill walking over a range of speeds," *Roy. Soc. Open Sci.*, vol. 5, no. 8, 2018, Art. no. 180550.
- [12] E. J. Park et al., "A hinge-free, non-restrictive, lightweight tethered exosuit for knee extension assistance during walking," *IEEE Trans. Med. Robot. Bionics*, vol. 2, no. 2, pp. 165–175, May 2020.
- [13] M. K. MacLean and D. P. Ferris, "Energetics of walking with a robotic knee exoskeleton," J. Appl. Biomech., vol. 35, no. 5, pp. 320–326, 2019.

- [14] Q. Li, M. Young, V. Naing, and J. M. Donelan, "Walking speed and slope estimation using shank-mounted inertial measurement units," in *Proc. IEEE Int. Conf. Rehabil. Robot.*, Jun. 2009, pp. 839–844.
- [15] A. M. López, D. Álvarez, R. C. González, and J. C. Álvarez, "Slope estimation during normal walking using a shank-mounted inertial sensor," *Sensors*, vol. 12, no. 9, pp. 11910–11921, 2012.
- [16] S. C. Sabatini, Martelloni, "Assessment of walking features from foot inertial sensing," *IEEE Trans. Biomed. Eng.*, vol. 52, no. 3, pp. 486–494, Mar. 2005.
- [17] C. Zou, R. Huang, J. Qiu, Q. Chen, and H. Cheng, "Slope gradient adaptive gait planning for walking assistance lower limb exoskeletons," *IEEE Trans. Automat. Sci. Eng.*, 2020. to be published, doi: 10.1109/TASE.2020.3037973.
- [18] C. Kim, Kim, "Real-time gait phase detection and estimation of gait speed and ground slope for a robotic knee orthosis," in *Proc. IEEE Int. Conf. Rehabil. Robot.*, 2015, pp. 392–397.
- [19] C. H. K. B. Shim, Han, "Terrain feature estimation method for a lower limb exoskeleton using kinematic analysis and center of pressure," *Sensors*, vol. 19, no. 20, 2019, Art. no. 4418.
- [20] G. Sup, Varol, "Upslope walking with a powered knee and ankle prosthetic: Initial results with an amputee subject," *IEEE Trans. Neural Syst. Rehabil. Eng.*, vol. 19, no. 1, pp. 71–78, Feb. 2011.
- [21] A. J. Young and L. J. Hargrove, "A classification method for user-independent intent recognition for transferoral amputees using powered lower limb prostheses," *IEEE Trans. Neural Syst. Rehabil. Eng.*, vol. 24, no. 2, pp. 217–225, Feb. 2016.
- [22] I. Kang, P. Kunapuli, and A. J. Young, "Real-time neural network-based gait phase estimation using a robotic hip exoskeleton," *IEEE Trans. Med. Robot. Bionics*, vol. 2, no. 1, pp. 28–37, Feb. 2020.
- [23] H. Huang, F. Zhang, L. J. Hargrove, Z. Dou, D. R. Rogers, and K. B. Englehart, "Continuous locomotion-mode identification for prosthetic legs based on neuromuscular-mechanical fusion," *IEEE Trans. Biomed. Eng.*, vol. 58, no. 10, pp. 2867–2875, Oct. 2011.
- [24] I. Kang, P. Kunapuli, H. Hsu, and A. J. Young, "Electromyography (emg) signal contributions in speed and slope estimation using robotic exoskeletons," in *Proc. IEEE 16th Int. Conf. Rehabil. Robot.*, 2019, pp. 548–553.
- [25] J.-Y. Jung, W. Heo, H. Yang, and H. Park, "A neural network-based gait phase classification method using sensors equipped on lower limb exoskeleton robots," *Sensors*, vol. 15, no. 11, pp. 27738–27759, 2015.
- [26] K. Seo et al., "RNN-based on-line continuous gait phase estimation from shank-mounted imus to control ankle exoskeletons," in Proc. IEEE 16th Int. Conf. Rehabil. Robot., 2019, pp. 809–815.
- [27] J. Yang et al., "Machine learning based adaptive gait phase estimation using inertial measurement sensors," in Proc. Des. Med. Devices Conf., Amer. Soc. Mech. Eng. Digit. Collection, 2019.
- [28] T. Bao, S. A. R. Zaidi, S. Xie, P. Yang, and Z.-Q. Zhang, "A cnn-lstm hybrid framework for wrist kinematics estimation using surface electromyography," *IEEE Trans. Instrum. Measurem.*, vol. 70, pp. 1–9, 2020, arXiv:1912.00799.
- [29] C. Ma, C. Lin, O. W. Samuel, L. Xu, and G. Li, "Continuous estimation of upper limb joint angle from semg signals based on scalstm deep learning approach," *Biomed. Signal Process. Control*, vol. 61, 2020. Art. no. 102024.
- [30] Y. Hu, Y. Wong, W. Wei, Y. Du, M. Kankanhalli, and W. Geng, "A novel attention-based hybrid cnn-rnn architecture for semg-based gesture recognition," *PLoS one*, vol. 13, no. 10, 2018, Paper e0206049.
- [31] D. Lee, B. J. McLain, I. Kang, and A. J. Young, "Biomechanical comparison of assistance strategies using a bilateral robotic knee exoskeleton," in *IEEE Trans. Biomed. Eng. (Under Review)*, IEEE, 2020.
- [32] C. L. Lewis and D. P. Ferris, "Invariant hip moment pattern while walking with a robotic hip exoskeleton," *J. Biomech.*, vol. 44, no. 5, pp. 789–793, 2011.
- [33] A. Krizhevsky, I. Sutskever, and G. E. Hinton, "Imagenet classification with deep convolutional neural networks," in *Proc. Adv. Neural Inf. Pro*cess. Syst., 2012, pp. 1097–1105.
- [34] C. M. Wall-Scheffler, "Sex Differences in incline-walking among humans," (in English), Integr Comp Biol, vol. 55, no. 6, pp. 1155-1165, Dec 2015, doi: 10.1093/icb/icv072.
- [35] J. Camargo, A. Ramanathan, W. Flanagan, and A. Young, "A comprehensive, open-source dataset of lower limb biomechanics in multiple conditions of stairs, ramps, and level-ground ambulation and transitions," *J. Biomech.*, vol. 119, 2021, Art. no. 110320.
- [36] D. A. Winter, "Kinematic and kinetic patterns in human gait: Variability and compensating effects," *Hum. Movement Sci.*, vol. 3, no. 1-2, pp. 51–76, 1984